

Published in final edited form as:

Int J Radiat Oncol Biol Phys. 2007 July 1; 68(3): 650–653. doi:10.1016/j.ijrobp.2007.02.011.

Direct Measurement of Lung Motion using Hyperpolarized Helium-3 MR Tagging

Jing Cai, Ph.D.¹, G. Wilson Miller, Ph.D.², Talissa A. Altes, M.D.^{2,3}, Paul W. Read, M.D., Ph.D.¹, Stanley H. Benedict, Ph.D.¹, Eduard E. de Lange, M.D.², Gordon D. Cates, Ph.D.⁴, James R. Brookeman, Ph.D.², John P. Mugler III, Ph.D.², and Ke Sheng, Ph.D.^{1,*}

¹Department of Radiation Oncology, University of Virginia, Charlottesville, VA, USA

²Department of Radiology, University of Virginia, Charlottesville, VA, USA

³Department of Radiology, Children's Hospital of Philadelphia, Philadelphia, PA, USA

⁴Department of Physics, University of Virginia, Charlottesville, VA, USA

Abstract

Purpose—To measure lung motion between end-inhalation and end-exhalation using a hyperpolarized helium-3 (HP ³He) magnetic resonance (MR) tagging technique.

Methods and material—Three healthy volunteers underwent MR tagging studies after inhalation of 1L HP ³He gas diluted with nitrogen. Multiple-slice 2D and volumetric 3D MR tagged images of the lungs were obtained at end-inhalation and end-exhalation, and displacement vector maps were computed.

Results—The grids of tag lines in the HP ³He MR images were well defined at end-inhalation and remained evident at end-exhalation. Displacement vector maps clearly demonstrated the regional lung motion and deformation that occurred during exhalation. Discontinuity and differences in motion pattern between two adjacent lung lobes were readily resolved.

Conclusions—HP ³He MR tagging technique can be used for direct *in vivo* measurement of respiratory lung motion on a regional basis. This technique may lend new insights into the regional pulmonary biomechanics and thus provide valuable information for the deformable registration of lung.

Keywords

Lung motion; Deformable registration; Hyperpolarized helium-3; MR tagging

INTRODUCTION

Deformable image registration has become a vital methodology among the emerging motion management methods for the purpose of time-encoded 4D radiation therapy. Numerous methods have been proposed to model lung deformation (1-5). However, validation of these

© 2007 Elsevier Inc. All rights reserved.

*Please send all correspondence and reprint requests to Department of Radiation Oncology University of Virginia BOX 800375 Charlottesville, VA 22908 Phone: 434-243-0030 Fax: 434-982-3520 ks2mc@virginia.edu.

Publisher's Disclaimer: This is a PDF file of an unedited manuscript that has been accepted for publication. As a service to our customers we are providing this early version of the manuscript. The manuscript will undergo copyediting, typesetting, and review of the resulting proof before it is published in its final citable form. Please note that during the production process errors may be discovered which could affect the content, and all legal disclaimers that apply to the journal pertain.

methods has been hampered by the lack of methodologies for direct *in vivo* measurement of organ motion. Proton (^1H) magnetic resonance (MR) tagging is a technique to generate a spatially-encoded pattern on tissue and subsequently monitor the tissue movement *in vivo*. This technique has been widely used for the assessment of the motion and deformation of myocardial tissue (6, 7). The application of ^1H MR tagging in assessing pulmonary mechanics has also been reported (8, 9), but the low proton density and numerous magnetic-susceptibility interfaces in the lung result in a low MR signal that limits the quality of information obtained with this technique. Hyperpolarized helium-3 ($\text{HP } ^3\text{He}$) is a gaseous MR contrast agent that, when inhaled, provides a very high signal from the lung airspaces (10-12). Furthermore, within the lung, ^3He has relatively long relaxation times and is less affected by susceptibility interfaces than protons (11). Thus, $\text{HP } ^3\text{He}$ appears to be an ideal species for creating tagged MR lung images. In the work presented here, an $\text{HP } ^3\text{He}$ MR tagging technique was developed that acquires images of human lungs at end-inhalation and end-exhalation in a single acquisition. A semi-automated tracking algorithm was developed to monitor the motion of each tissue element defined by the grid of tags, permitting the measurement of displacement vectors corresponding to the motion between the two respiratory phases.

METHODS AND MATERIALS

$\text{HP } ^3\text{He}$ MR tag imaging was performed in three healthy volunteers (1 male, 2 female, ages 32, 25 and 29). The study was approved by our institutional review board. All studies were performed on a 1.5T MR scanner (Magnetom Sonata, Siemens, Malvern, PA), and ^3He gas was polarized to approximately 40% using a commercial system (Model 9600 Helium Polarizer, MITI, Durham, NC). Following inhalation of a 1L mixture of ~400 ml $\text{HP } ^3\text{He}$ and ~600 ml N_2 , tagging grids were created at breath hold, by spatially selectively tipping down ^3He magnetizations in a 2D or 3D grid pattern (13). Tag spacing was set to be 18-22 mm, large enough to prevent ^3He gas diffusion from obscuring the tagging grid during the scan. A gradient-echo MR pulse sequence (TR/TE, 1.9/0.6 ms; FOV, 320-360×260-315 mm; matrix, 56×64; flip angle, 5°; and slice thickness, 30 mm) was subsequently used to acquire two sets of tag images: the first immediately following application of the tag pattern (end-inhalation) and the second 2-3 seconds later after the subject had exhaled (end-exhalation). For the 3D tag imaging, 22 partitions with a slice thickness of 9 mm were used.

Raw images were interpolated by a factor of 3 to improve the definition of tags. Grid peaks were located and analyzed using a semi-automated image reconstruction and processing procedure implemented in MATLAB (The MathWorks, Natick, MA), with occasional manual intervention when the tagging grids shifted out of the imaging plane, overlapped with other grids, or were corrupted by the pulmonary bronchi. Displacement vectors were computed from the observed motion of the grid peaks.

RESULTS

The 2D tagging grids were very well defined in the $\text{HP } ^3\text{He}$ MR images at end-inhalation (Fig. 1a, d), and remained quite visible, although deformed by the intervening lung movement, at expiration (Fig. 1b, e). The grids are somewhat blurred and rounded in shape primarily due to fast ^3He diffusion and interpolation of low-resolution raw images. The images at end-exhalation visibly illustrate the regional lung deformation of the tags that occurred between two respiratory phases. Some grid elements, particularly along the fissure between two lung lobes, appeared to move relative to each other creating a shear effect presumably due to the different motion pattern of the two lobes (arrows).

Fig. 1c, f shows the 2D maps of the corresponding displacement vector maps. As expected, the largest displacement is in the lung bases adjacent to the diaphragm. The shear effect of motion is evident in the displacement maps, especially in the sagittal plane where a longer inter-lobe fissure exists. Fig. 1f clearly depicted the difference in the motion pattern between the superior lobe and the inferior lobe. The corresponding distributions of the displacement vectors (length and direction), as shown in Fig. 2, revealed that the superior lobe moves greater (mean length: 30.6 mm) and primarily in the craniocaudal direction (mean direction: 66.3°), while the inferior lobe moves relatively less (mean length: 18.0 mm) and primarily in the anterior-posterior direction (mean direction: 6.4°).

Fig. 3 shows the surface rendered 3D HP ^3He tagged images of the lungs (a) at end-inhalation (golden) and at end-exhalation (blue) and the corresponding 3D displacement vectors (b). Movement of the 3D tagging grids is apparent between the two respiratory phases. 3D displacement showed regional motion differences in adjacent lung grids, and revealed a twisting effect of motion in the middle and lower regions of the left lung (right side of the image). Possible causes of the twisting are the cardiac motion and the difference in the frictional forces that the interior lung region and the posterior lung region are experiencing during breathing.

DISCUSSION

In this paper, we reported an HP ^3He tagging MRI technique that permits direct *in vivo* measurement of lung motion and deformation on a regional basis between two respiration phases. We found that the majority of the tagging grids remained discernible at expiration, and deformed due to the intervening motion of the lung tissue. This technique has great promise in solving one of the most challenging questions in advanced motion management of lung tumor radiotherapy: the validation of deformable registration, which may yield an infinite number of solutions and is intrinsically ambiguous. Compared to 4D-CT and other cine imaging modalities, HP ^3He MR tagging of lungs carries tracking information that is unambiguously encoded in the grids. Our preliminary results revealed a discontinuity between two adjacent lobes that is not considered in current deformable registration modeling. Furthermore, HP ^3He tagging images provide hundreds of control points (tagging grids) that considerably reduce the number of freedoms for deformable registration, and therefore can largely eliminate the ambiguity.

The accuracy of the HP ^3He grid-tagging technique is reduced by any effect other than lung motion that causes distortion of the tags. Measurement error is expected at lung boundaries due to the irregular shape of the tissue grid elements. In addition, the loss of tagging grids was observed after exhalation near large pulmonary bronchi and in anterior lung regions. Furthermore, data processing (interpolation, filtering and thresholding) could have introduced some error in the determination of grid-element positions.

One extension of this work is to increase the temporal resolution of image acquisition using fast MR imaging techniques (14), which allows acquiring dynamic images of tagged lung motion throughout the breathing cycle and can potentially reveal the nonlinear effect of lung motion such as hysteresis. Reducing the imaging time will also reduce the sensitivity to diffusive motion of the inhaled ^3He gas, enabling the use of smaller tag spacing, and thereby increasing the spatial resolution of the displacement maps. With the optimization of spatial/temporal resolution and the improvement of automatic 3D tag tracking, we anticipate establishing a gold standard of lung deformation based on the HP ^3He MR direct measurement that can be used to improve current deformable registration methods.

CONCLUSIONS

An HP ^3He tagging technique was validated in healthy volunteers for direct measurement of lung motion between two respiratory phases. This technique may lend new insights into the complexities of regional pulmonary mechanics and provide valuable information for improving deformable image registration methods of the lungs.

Acknowledgments

This work was supported by an NIH grant R01-HL079077 from the National Heart, Lung, and Blood Institute, grant IN2002-01 from the Commonwealth of Virginia Technology Research Fund, and Siemens Medical Solutions.

REFERENCES

1. Brock KK, Sharpe MB, Dawson LA, et al. Accuracy of finite element model-based multi-organ deformable image registration. *Med Phys.* 2005; 6:1647–1659. [PubMed: 16013724]
2. Zhang T, Orton NP, Tome WA. On the automated definition of mobile target volumes from 4D-CT images for stereotactic body radiotherapy. *Med Phys.* 2005; 11:3493–3502. [PubMed: 16370433]
3. Keall PJ, Joshi S, Vedam SS, et al. Four-dimensional radiotherapy planning for DM-LC-based respiratory motion tracking. *Med Phys.* 2005; 4:942–951. [PubMed: 15895577]
4. Pevsner A, Davis B, Joshi S, et al. Evaluation of an automated deformable image matching method for quantifying lung motion in respiration-correlated CT images. *Med Phys.* 2006; 2:369–376. [PubMed: 16532942]
5. Wang H, Lei D, O'Daniel J, et al. Validation of an accelerated 'demons' algorithm for deformable image registration in radiation therapy. *Phys Med Biol.* 2005; 12:2887–2905. [PubMed: 15930609]
6. Zerhouni EA, Parish DM, Rogers WJ, et al. Tagging with MR imaging: a method for noninvasive assessment of myocardial motion. *Radiology.* 1988; 169:59–63. [PubMed: 3420283]
7. Axel L, Dougherty L. Imaging of motion with spatial modulation of magnetization. *Radiology.* 1989; 171:841–845. [PubMed: 2717762]
8. Chen Q, Mai VM, Bankier AA, et al. Ultrafast MR grid-tagging sequence for assessment of local mechanical properties of the lungs. *Magn Reson Med.* 2001; 45:24–28. [PubMed: 11146481]
9. Voorhees A, An J, Berger KI, et al. Magnetic resonance imaging-based spirometry for regional assessment of pulmonary function. *Magn Reson Med.* 2005; 54:1146–1154. [PubMed: 16217776]
10. Kauczor HU, Hofmann D, Kreitner KF, et al. Normal and abnormal pulmonary ventilation: visualization at hyperpolarized He-3 MR imaging. *Radiology.* 1996; 201:564–568. [PubMed: 8888259]
11. de Lange EE, Mugler JP 3rd, Brookeman JR, et al. Lung air spaces: MR imaging evaluation with hyperpolarized ^3He gas. *Radiology.* 1999; 210:851–857. [PubMed: 10207491]
12. Moller HE, Chen XJ, Saam B, et al. MRI of the lungs using hyperpolarized noble gases. *Magn Reson Med.* 2002; 47:1029–1051. [PubMed: 12111949]
13. Cai J, Altes TA, Miller GW, et al. MR grid-tagging using hyperpolarized helium-3 for quantitative assessment of regional pulmonary biomechanics. *Proc ISMRM.* 2006; 864
14. Salerno M, Altes TA, Brookeman JR, et al. Dynamic spiral MRI of pulmonary gas flow using hyperpolarized ^3He : Preliminary studies in healthy and diseased lungs. *Magn Reson Med.* 2001; 54:667–677. [PubMed: 11590642]

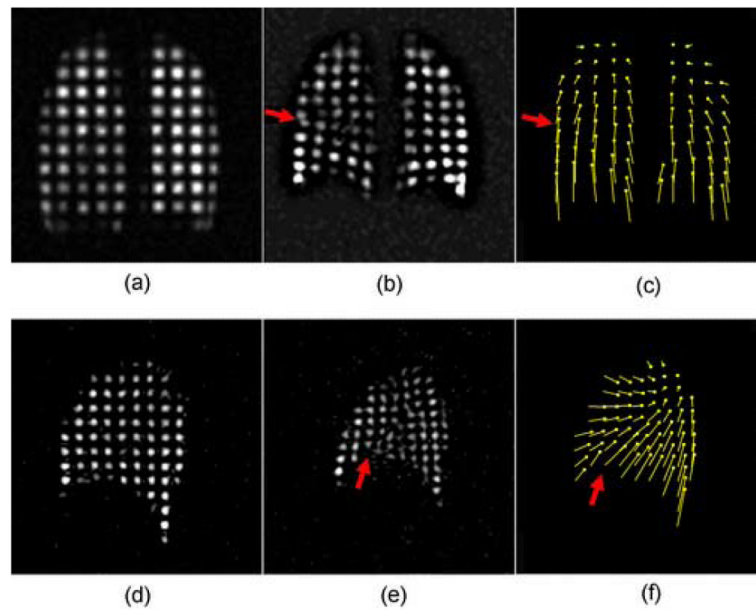


Fig. 1.

Representative slices of 2D HP ^3He grid-tagged MR images of the lung, acquired from healthy volunteers in the coronal (a, b) and sagittal planes (d, e) at end-inhalation (a, d) and at end-exhalation (b, e), with the corresponding displacement maps (c, f). The tail of each displacement vector indicates the position of the associated tissue grid element at end-inhalation and the solid round head indicates the position at end-exhalation. The coronal plane was from the posterior lung region and the sagittal plane was from the middle right lung region. Tag spacing was 22 mm and 18 mm in the coronal and sagittal images respectively. Sliding motion effect was observed at the fissure between the superior lobe and inferior lobe in both the MR tagging images and the displacement maps (red arrows).

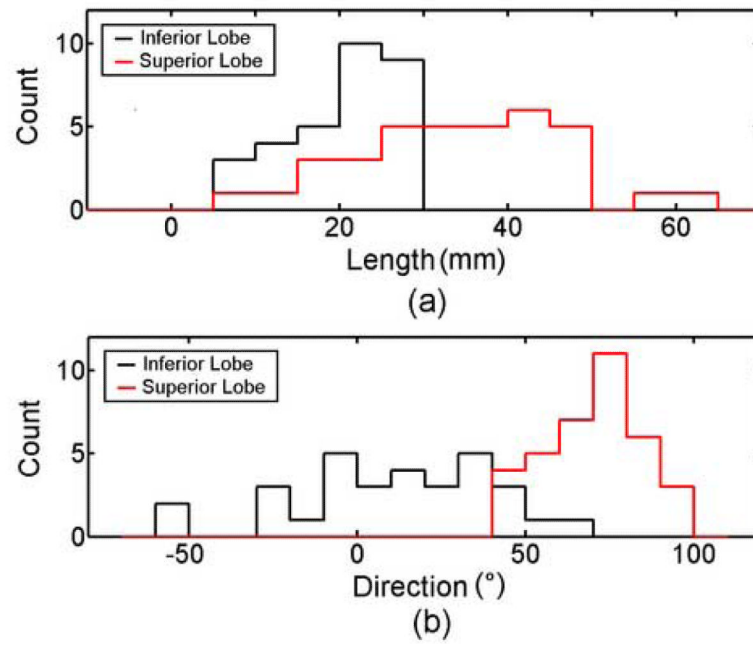


Fig. 2. Distributions of displacement vectors (length and direction) for the interior lobe and the superior lobe correspond to Fig. 1f. Direction is defined as 0° is the horizontal direction point to the left and 90° is the vertical direction point to the top.

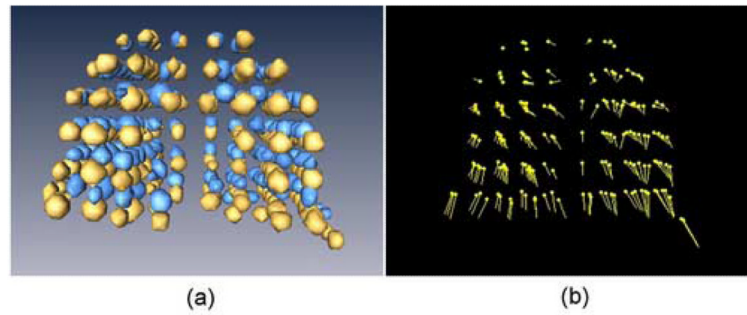


Fig. 3. Surface rendering of 3D tagging grid peaks (a) and the corresponding 3D displacement vectors (b). MR HP ^3He tagged lung images were obtained at end-inhalation (golden) and at end-exhalation (blue), showing the distribution of the tagging grid throughout the lung. The tail of each displacement vector indicates the position of the associated tissue grid element at end-inhalation and the solid round head indicates the position at end-exhalation.